International Journal of Mechanical, Industrial and Aerospace Sciences
ISSN: 2517-9950
Vol:5, No:7, 2011

Numerical Study of Hypersonic Glide Vehicle based on Blunted Waverider

Liu Jian-xia, Hou Zhong-xi and Chen Xiao-qing

***Abstract*—**The waverider is proved to be a remarkably useful configuration for hypersonic glide vehicle (HGV) in terms of the high lift-to-drag ratio. Due to the severe aerodynamic heating and the processing technical restriction, the sharp leading edge of waverider should be blunted, and then the flow characteristics and the aerodynamic performance along the trajectory will change. In this paper, the flow characteristics of a HGV, including the rarefied gas effect and transition phenomenon, were studied based on a reference trajectory. A numerical simulation was carried out to study the performance of the HGV under a typical condition.

***Keywords*—**Aerodynamic, CFD, Thermodynamic, Waverider

I. Introduction

HYPERSONIC Glide Vehicle has been a hot topic in the aerospace area in terms of the high speed and long range performances [1]–[3]. Due to the high lift-to-drag ratio in hypersonic flow, the waverider is proved to be a remarkable basic configuration for HGV. The waverider which is designed with a theory infinitely sharp leading edge will lead to an infinite value of the temperature. In order to decrease the aerodynamic heating on the surface, the sharp leading edge needs to be blunted, and then the flow characteristics and the aerodynamic performance might change. Reference [4]–[8] studied the rarefied gas effect of hypersonic vehicles, and presented some methods to calculate the aerodynamic performance in the rarefied region. Based on the wind tunnel experiment and flight data, [9]–[13] studied the transition phenomena in hypersonic flows around flat plate, swept cylinder and cone, and summarized series of transition criteria. Reference [14]–[24] validated the high lift-to-drag ratio characteristic of a waverider in hypersonic flow by means of estimation, CFD and experiment methods. In this paper, coupled with the glide trajectory and blunted waverider configuration, we studied the flow characteristics of a HGV, including the rarefied gas effect and transition phenomenon along the reference glide trajectory. Based on these analyses, the vehicle's aerodynamic and thermodynamic performances under a typical condition were obtained using CFD method.

LIU Jian-xia, Ph.D candidate, College of Aerospace and Material Engineering, National University of Defense Technology, Changsha, 410073, China (e-mail: liujianxia2002@126.com)

HOU Zhong-xi , professor , College of Aerospace and Material Engineering, National University of Defense Technology, Changsha, 410073, China (e-mail: cn_hzx@sina.com)

CHEN Xiao-qing, Ph.D candidate, College of Aerospace and Material Engineering, National University of Defense Technology, Changsha, 410073, China (e-mail: gkbatchelor@gmail.com)

This work is financially supported by National Natural Science Foundation of China (Grant No. 90916016) and Hunan Provincial Innovation Foundation for Postgraduate (Grant No. B110102).

II. Configuration Based on Blunted Waverider

The waverider is hypersonic configuration which is designed to have shock wave attached to the leading edge of the vehicle, thus preventing the high pressure behind the shock wave to leak from the lower surface to the upper surface. In this paper, the basic waverider is generated from a reference flow field around a hypersonic cone using the method in [25]. The design Mach number is 10, the cone's half-angle is 12^{o}, the length is 3.5m, and the divergence angle is 45^{o}. The sharp leading edge of original waverider is blunted with 3cm, which is calculated with Fay-Riddell formula for aerodynamic heating, as shown in Fig. 1.

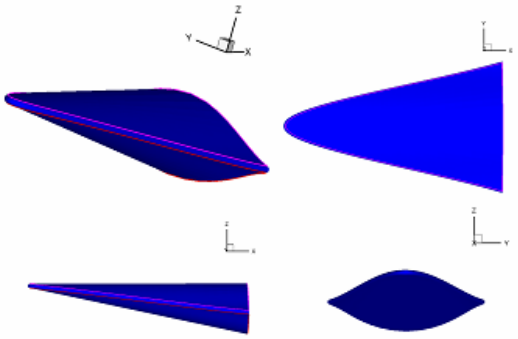

Fig. 1 The configuration of the hypersonic glide vehicle

III. Flow Characteristics on Glide Trajectory

Because of the good aerodynamic performance of waverider configuration, HGV's trajectory is different from conventional vehicles, such as hypersonic reentry missile and manned spacecraft. Fig. 2 gives one reference trajectory of hypersonic glide vehicle. We can see that the values of height and velocity are fluctuating with time along the glide trajectory. The flow characteristics of the HGV along the trajectory might be changed. Based on the reference trajectory and the basic configuration shown in Fig. 1, we investigate the typical flow characteristics of the HGV, including the rarefied gas effect and transition phenomenon.

A. Rarefied Gas Effect

In Fig. 2, we can see that the HGV flies in a large height range from the ground to the altitude of 165 km. When the vehicle flies at high altitude, the assumption of continuous flow

is not reasonable any more. In order to confirm the flow mechanism and boundary conditions for the HGV at each altitude, it is necessary to separate the rarefied region from the continuum flow. One parameter that characterizes rarefied gas effect is the Knudsen number, which is the ratio of molecular mean free path to a characteristic length. It can be calculated as below [4]:

$$Kn = 1.26 \times \sqrt{\gamma} \times \frac{M_\infty}{\mathrm{Re}_\infty} \times \frac{L}{\delta} \quad (1)$$

where γ is the specific heat ratio of air, M_∞ is the Mach number of free stream, Re_∞ is the Reynolds number, L is the characteristic length, and δ is the thickness of boundary layer. Once the Knudsen number is greater than 0.01, the rarefied gas effect should be considered.

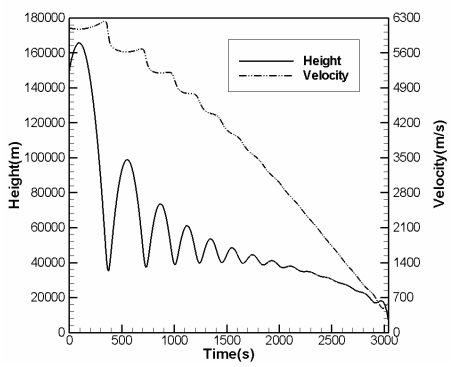

Fig. 2 Height and velocity varied with time

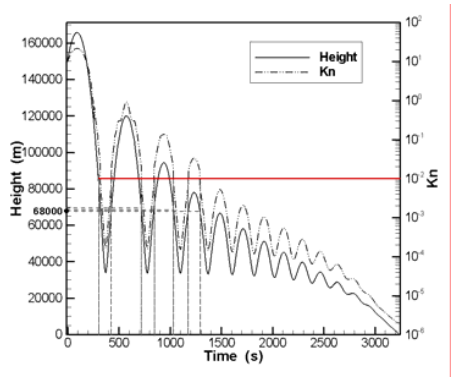

Fig. 3 Knudsen number and height varied with time

As shown in Fig. 3, if the altitude is higher than 68 km, the Knudsen number is always higher than 0.01, the assumption of continuous flow is not reasonable any more. It means that the rarefied gas effect should be considered for the HGV if the vehicle flies above 68km. We also note that the density of atmosphere is less than $10^{-5}\mathrm{kg/m}^3$ when the altitude is higher than 68km; the aerodynamic heating of the HGV is not serious in this region. More attention should be paid to the trajectory where the altitude is lower than 68km.

B. Transition phenomenon

In the hypersonic flow field, the convective heat transfer is very serious when the flow is turbulent. It is necessary for us to study the transition phenomenon for the HGV based on blunted waverider configuration before numerical simulation.

Based on the wind tunnel experiment data, [9]–[12] studied the transition phenomena in hypersonic flow and summarized series of transition criteria. The transition Reynolds number of Sheets [13] shows a better agreement with the flight data and the e^N method than others. The relation can be expressed as:

$$\mathrm{Re}_{trL} = 6400 \times (M_e)^{3.66} \quad (2)$$

where M_e is the edge Mach number.

Using (2), we study the transition phenomena on the surfaces of the HGV with more attention to the moment when the vehicle's speed is hypersonic. Fig. 4 shows the transition Reynolds number and the local Reynolds number by the characteristic size of the HGV's length on the upper surface. Note that the transition Reynolds number is greater than the local Reynolds number on the upper surface almost all the time. So we treat the flow of upper surface as laminar in this paper.

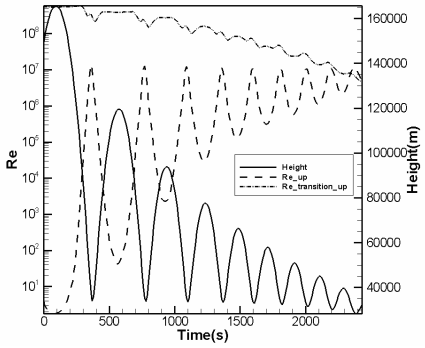

Fig. 4 Transition analysis on the upper surface

The transition Reynolds number and the local Reynolds number on the HGV's lower surface are shown in Fig. 5. Fig. 5 (a) gives the local Reynolds number by the characteristic size of the HGV's length, and Fig. 5(b) gives the local Reynolds number by the characteristic size with half of the HGV's length. We can note that the transition Reynolds number is greater than the local Reynolds number on the lower surface at most of the time. The lower surface is always wetted by laminar flow unless the vehicle is at the nadir of the glide trajectory.

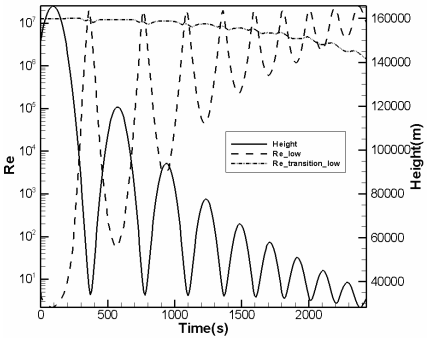

(a) Characteristic size with the HGV's length

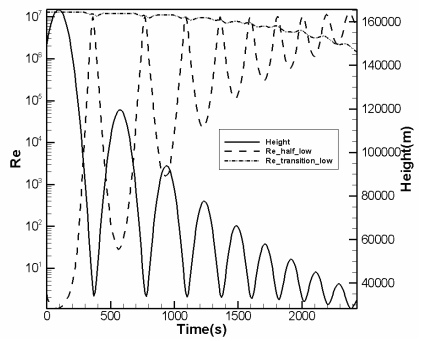

(b) Characteristic size with half of the HGV's length

Fig. 5 Transition analysis on the lower surface

IV. Numerical Method

In this section, the numerical method used in this paper is introduced.

The governing equations for the steady-state full Navier-Stokes equations in conservation form [25] are:

$$\frac{\partial U}{\partial t}+\frac{\partial (E_i-E_v)}{\partial x}+\frac{\partial (F_i-F_v)}{\partial y}+\frac{\partial (G_i-G_v)}{\partial z}=S \tag{3}$$

where the subscript i denotes the term that appears in the equations of motion for inviscid flow, and the subscript v denotes the term of the viscous flux vectors, i.e., terms unique to the equations of motion when the viscous and the heat-transfer effects are included. The vector of the chemical source terms is represented by S. Because chemical reactions are not involved here, S is set to zero. If written in vector form, the governing equations would be:

$$U=\left[\rho,\rho u,\rho v,\rho w,\rho e\right]^{\mathrm{T}}$$

$$E_i=\begin{bmatrix}\rho u\\ \rho u^2+p\\ \rho uv\\ \rho uw\\ (\rho e_t+p)u\end{bmatrix},\ E_v=\begin{bmatrix}0\\ \tau_{xx}\\ \tau_{xy}\\ \tau_{xz}\\ u\tau_{xx}+v\tau_{xy}+w\tau_{xz}+q_x\end{bmatrix}$$

$$F_i=\begin{bmatrix}\rho v\\ \rho uv\\ \rho v^2+p\\ \rho vw\\ (\rho e_t+p)v\end{bmatrix},\ F_v=\begin{bmatrix}0\\ \tau_{xy}\\ \tau_{yy}\\ \tau_{yz}\\ u\tau_{yx}+v\tau_{yy}+w\tau_{yz}+q_y\end{bmatrix}$$

$$G_i=\begin{bmatrix}\rho w\\ \rho uw\\ \rho vw\\ \rho w^2+p\\ (\rho e_t+p)w\end{bmatrix},\ G_v=\begin{bmatrix}0\\ \tau_{xz}\\ \tau_{yz}\\ \tau_{zz}\\ u\tau_{zx}+v\tau_{zy}+w\tau_{zz}+q_z\end{bmatrix}$$

where

$$\tau_{xx}=2\mu\frac{\partial u}{\partial x}-\frac{2}{3}\mu\nabla\cdot V,$$

$$\tau_{yy}=2\mu\frac{\partial v}{\partial y}-\frac{2}{3}\mu\nabla\cdot V,$$

$$\tau_{zz}=2\mu\frac{\partial w}{\partial z}-\frac{2}{3}\mu\nabla\cdot V,$$

$$\tau_{xy}=\tau_{yx}=\mu\left(\frac{\partial u}{\partial y}+\frac{\partial v}{\partial x}\right),$$

$$\tau_{zx}=\tau_{xz}=\mu\left(\frac{\partial u}{\partial z}+\frac{\partial w}{\partial x}\right),$$

$$\tau_{yz}=\tau_{zy}=\mu\left(\frac{\partial v}{\partial z}+\frac{\partial w}{\partial y}\right),$$

$$q_x=k\frac{\partial T}{\partial x},$$

$$q_y=k\frac{\partial T}{\partial y},$$

$$q_z=k\frac{\partial T}{\partial z},$$

$$e_t=\frac{p}{(\gamma+1)\rho}+\frac{1}{2}\left(u^2+v^2+w^2\right)$$

where μ is the coefficient of viscosity which can be calculated by Sutherland law:

$$\mu=1.485\times10^{-6}\frac{T^{1.5}}{T+110.4} \tag{4}$$

and k denotes thermal conductivity which is determined by Prandtl number:

$$k=\frac{\mu C_p}{\mathrm{Pr}} \tag{5}$$

The governing equations are discretized and numerically integrated based on a finite-volume approach. Inviscid flux is calculated by AUSM+ scheme, and the viscous flux is calculated by the central difference scheme. Euler backward difference method with fully implicit scheme is used for temporal integration. The wall boundary conditions are consist of a non-slip condition, a zero pressure gradient condition normal to the surface and a radiative wall with the emissivity of 0.8 which is the average value of silicon carbide coating material. Inflow boundary conditions are fixed with the values of free stream, and outflow boundary conditions are obtained using 1st extrapolation. The grid convergence study in [26] showed that heat flux in hypersonic flow would converge if the value of cell Reynolds number is less than or equal to 3.

In order to verify the algorithm described above, a case with experiment data [22] is chosen and simulated in this paper, which is a hypersonic viscous flow field around a cylinder. The computational condition is shown in TABLE I.

TABLE I
Computational Condition of the Varified Case

R(m)	Ma_∞	P_∞(N/m^2)	T_∞(K)	T_w(K)
0.038	16.34	82.95	52	294.4

As shown in Fig. 6, the experiment data of stagnation heat transfer is about $5.90\times10^5\,\mathrm{W/m^2}$ while CFD result is $5.93\times10^5\,\mathrm{W/m^2}$. The CFD result is in a good agreement with the experimental data along the wall, which shows that the numerical method used in the paper would be appropriate for the flow simulation of the HGV.

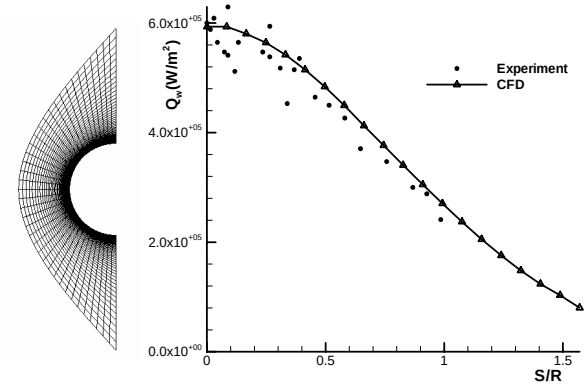

Fig. 6 Grid and result for the verified case

V. Computational Results and Discussion

A. Flow condition

Based on the analysis results above, we decide to make an in-depth study on the aerodynamic and thermodynamic performance of the HGV under a typical flow condition which is shown in TABLE II. Under this condition, the entire surfaces of the HGV are wetted by the laminar flow. As shown in Fig. 7, the computational grid is generated based on the rule of [26].

TABLE II
Computational condition of the HGV

H(km)	V(m/s)	α (°)	P(N/m^2)	T(K)
40	3171.89	2	287.144	250.35

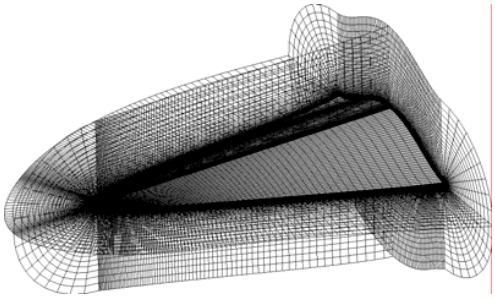

Fig. 7 Computational grid for hypersonic glide vehicle

B. Aerodynamic performance

The pressure contours is shown in Fig. 8. Because of the blunt leading edge, we can see that a well defined bow shock structure surrounding the entire vehicle is formed. The air leaks out from the lower surface to the upper surface along the leading edge. The pressure around the nose is much higher than other region.

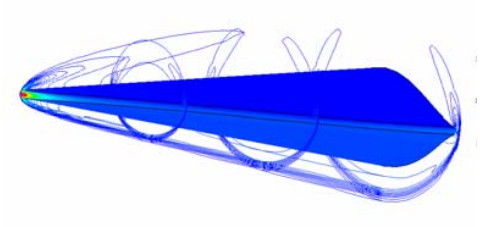

Fig. 8 Pressure contours around the HGV

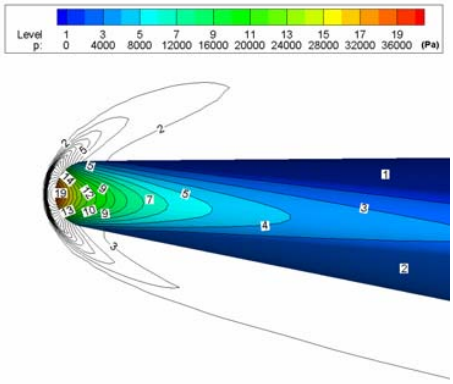

Fig. 9 Pressure Distribution of the nose region

Fig. 9 shows the pressure distribution in the nose region. We can see that the bow shock stands off the leading edge by some distance and allows high pressure air to spill from the lower surface to the upper surface, which would reduce the lift, increase the drag, and then decrease the overall aerodynamic efficiency of the HGV. As shown in Fig. 10, the shock distance calculated by the Billig's correlations for sphere-cone shapes is 0.1477R, and for cylinder-wedge shapes is 0.4045R. The shock distance simulated in this paper of the HGV is between 0.1477R and 0.4045R. The result indicates that the flow of the nose region can not be simply regarded as the flow around a cylinder or sphere with a same radius, and the correction should be added. More attention should be paid to the flow mechanism of this region. Fig. 11 shows the pressure distribution of the cross-section. It is clear to see that the pressure on the lower surface is much higher than the upper surface, which is one of the most important factors to retain the high lift performance for the HGV though the air leaks from the leading edge.

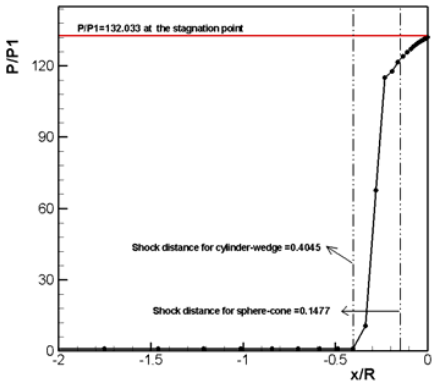

Fig. 10 Pressure distributions along the stagnation line

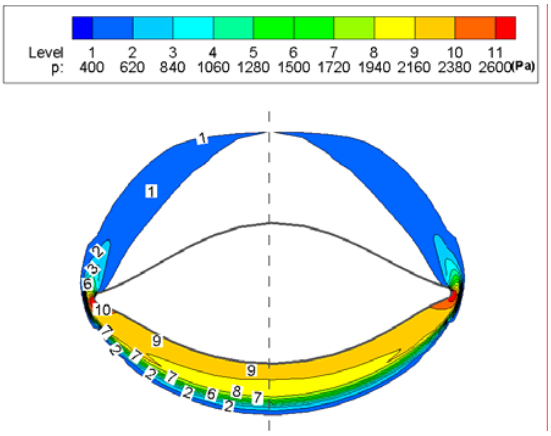

Fig. 11 Pressure distribution at the bottom

In TABLE III, the aerodynamic coefficient of the HGV is listed in detail. Almost all lift is contributed by the high pressure on lower surface. As to the drag, the inviscid force occupies 91.4%, in which the blunt leading edge, the upper and lower surfaces contribute 21.767%, 0.063%, 69.57%, respectively. The blunt leading edge has a significant influence on the inviscid drag of the HGV. As to the viscous drag, the blunt leading edge, the upper and lower surfaces contribute 2.29%, 2.06%, 4.25%, respectively. Then the lift-to-drag ratio is calculated to be 2.69.

Though the aerodynamic performance of the HGV is decreased after blunted, the lift-to-drag ratio obtained in this paper is proved to be enough for the need of glide trajectory [27].

TABLE III
AERODYNAMIC PERFORMANCE OF THE HGV ($S=8.0482m^2$)

	Lift Coefficient (/Total Lift Coefficient)	Drag Coefficient (/Total Drag Coefficient)	
		Inviscid	Viscous
Leading Edge	0.001221 (2.87%)	0.003444 (21.767%)	0.0003627 (2.29%)
Upper Surface	-0.0078946 (-18.53%)	0.000011 (0.063%)	0.0003254 (2.06%)
Lower Surface	0.049276 (115.66%)	0.011013 (69.57%)	0.0006732 (4.25%)
Total	0.0426024 (100%)	0.014468 (91.4%)	0.0013613 (8.6%)
		0.0158293 (100%)	

C. Thermodynamic performance

The heat flux on the surfaces of the HGV is shown in Fig. 12. Note that the heat transfer on the surface is lower than leading edge. Though the heat flux is about $9.0\times10^5 W/m^2$ at the stagnation point of the HGV, the heat flux on the surface is less than $5.0\times10^4 W/m^2$ and 80% of the leading edge is less than $2.625\times10^5 W/m^2$. Fig. 13 gives the radiative equilibrium temperature distribution on the vehicle, including the upper surface, lower surface and the leading edge. The temperature of upper surface ranges from 700K to 1000K, and the lower surface is between 900K and 1200K. Meanwhile, the range of most leading edge is from 1400K to 1500K, and the temperature of the nose region is about 2000K.

Based on the analysis above, the heat transfer of the HGV is not serious except the nose region near the stagnation point. To face the high temperature at the nose region, we can use carbon-carbon to fabricate the nose.

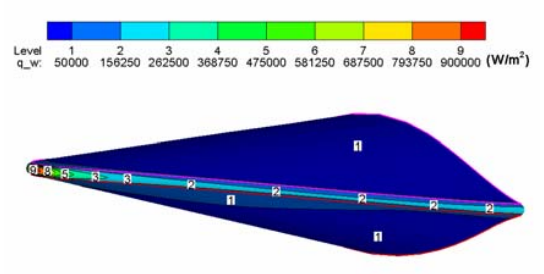

Fig. 12 Heat Flux on the surfaces of hypersonic glide vehicle

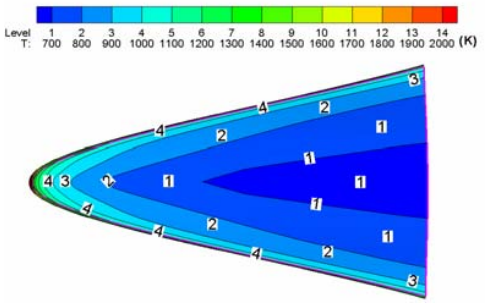

(a) The upper surface

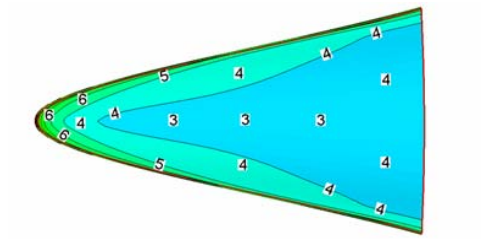

(b) The lower surface

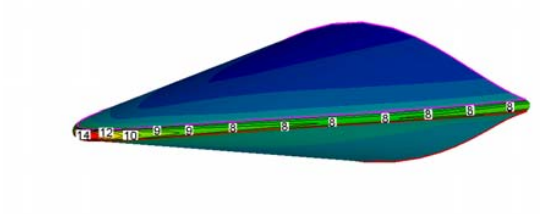

(c) The leading edge

Fig. 13 Temperature on the surfaces of hypersonic glide vehicle

VI. CONCLUSIONS

To study the performance of hypersonic glide vehicle which is based on the waverider configuration with blunt leading edge, this paper analyzed the flow characteristic of a HGV, including the rarefied gas effect and transition phenomenon along the trajectory. The aerodynamic and thermodynamic performances were studied by numerical simulation.

The hypersonic glide vehicle based on blunted waverider retains the high lift-to-drag ratio, and the heat transfer on the surfaces of a HGV is not serious except the nose region near the stagnation point. Waverider configuration remains a valuable candidate for hypersonic glide vehicle though the leading edge is blunted.

Further work will be focused on the flow mechanism of nose region, the blunt method for hypersonic glide vehicle and the detailed design of temperature protection system.

REFERENCES

[1] Y. Sun, H. P. Zhao, "Application analysis and prospects of near-space vehicles," Signal and Information, vol. 138, no. 110, 2008, pp. 26-28.(in Chinese)
[2] R. T. Voland, L. D. Huebner, C. R. Mcclinton, "X-43A hypersonic vehicle technology development," Acta Astronautica, vol. 59, 2006, pp. 181-191.
[3] I. Dietlein, A. Kopp, "System analysis for 'sharp-edge' re-entry vehicles," in 16th AIAA/DLR/DGLR International Space Planes and Hypersonic Systems and Technologies Conference, 2009.
[4] Z. H. Qu, W. Liu, M. Zeng, J. Liu, "Hypersonic aerodynamics," NUDT press, 2001, pp. 206-222 (in Chinese)
[5] Z. H. Wang, L Bao, B. G. Tong, "Variation character of stagnation point heat flux for hypersonic pointed bodies from continuum to rarefied flow states and its bridge function study," Sci China Ser G, vol. 39, no. 8, 2009, pp. 1134-1140.
[6] R. L. Zhu, Y. H. Cao, " The hybrid code of adaptive local time step for DSMC PEPSM on the hypersonic vehicle," Acta Aerodynamica Sinica vol. 26, no. 3, 2009, pp. 394-399.
[7] V. V. Riabov, "Heat transfer on a hypersonic sphere with diffuse rarefied-gas injection," in 42nd AIAA Aerospace Sciences Meeting and Exhibit, Reno, Nevada, 2004.
[8] W. F. N. Santos, M. J. Lewis, "Aerodynamic heating performance of power law leading edges in rarefied hypersonic flow," in 36th AIAA Thermo physics Conference, Orlando, Florida, 2003.
[9] A. Jocksch, L. Kleiser, "Growth of turbulent spots in high-speed boundary layers on a flat plate," International Journal of Heat and Fluid Flow, vol. 29, 2008, pp. 1543-1557.
[10] E. Benard, R. K. Cooper, A. Sidorenko, "Transitional and turbulent heat transfer of swept cylinder attachment line in hypersonic flow," International Journal of Heat and Mass Transfer, vol. 49, 2006, pp. 836-843.
[11] S. P. Schneider, "Hypersonic laminar–turbulent transition on circular cones and scramjet forebodies," Progress in Aerospace Sciences, vol. 40, 2008, pp. 1-50.
[12] S. P. Schneider, "Flight data for boundary-layer transition at hypersonic and supersonic speeds," Journal of Spacecraft and Rockets, vol. 36, no. 1, 1999, pp. 8-20.
[13] N. Sheetz, "Ballistics range boundary layer transition measurements on cones at hypersonic speeds," Viscous Drag Reduction, 1968.
[14] D. O.Van mol, J. D. J. Anderson, "Heat transfer characteristics of hypersonic wave-riders with an emphasis on leading edge effects," AIAA92-2920.
[15] M. J.Lewis, M.Chauffour, "Shock-based waverider design with pressure gradient corrections and computational simulations," Journal of Aircraft, vol. 42, no. 15, 2005, pp. 1350-1352.
[16] Y. K. Wang, S. F. Yang, D. J. Zhang, X. Y. Deng. "Design of waverider configuration with high lift-drag ratio," Journal of Aircraft, vol. 44, no. 1, 2007, pp. 144-148.
[17] T. F. Zien, "Determination of surface pressure and temperature distributions on hypersonic waveriders," in 26th AIAA Applied Aerodynamics Conference, Honolulu, Hawaii, 2008.
[18] J. Che, S. Tang, "Research on integrated optimization design of hypersonic cruise vehicle," Aerospace Science and Technology. vol. 12, 2008, pp. 567-572.
[19] C. M. Di, M. Marini, B. S. Di, A. Schettino, G. Ranuzzi. "Numerical prediction of aerothermodynamic effects on a reentry vehicle body flap configuration," Acta Astronautica. vol. 65, 2009, pp. 221-239.
[20] J. Pan, C. Yan, Y.F Geng, J. Wu, "Aerothermodynamics of the waveriders applying artificially blunted leading edge concept," in 47th AIAA Aerospace Sciences Meeting Including the New Horizons forum, Orlando, Florida, 2009.
[21] X. Liu, X. G. Deng. "Application of high-order accurate algorithm to hypersonic viscous flows for calculating heat transfer distributions," in 45th AIAA Aerospace Sciences Meeting and Exhibit, Reno, Nevada: 2007.
[22] K. H. Kim, C. Kim, O. Hyun. "Methods for the accurate computations of hypersonic flows I: AUSMPW+ scheme," Journal of Computational Physics, vol. 174, 2001, pp. 38-80.
[23] J. H. Lee, O. H. Rho., "Numerical analysis of hypersonic viscous flow around a blunt body using Roe's FDS and AUSM+ schemes," AIAA paper 97-2054, 1997.
[24] R. Bur, B. Chanetz, "Experimental study on the PRE-X vehicle focusing on the transitional shock-wave/boundary-layer interactions," Aerospace Science and Technology, vol. 13, 2009, pp. 393-401.
[25] X. Q. Chen, "Research on aerodynamic design for hypersonic waverider vehicle," ChangSha, NUDT, 2006
[26] J. J. Bertin, R. M. Cummings, "Critical hypersonic aerothermodynamic phenomena," Annual Review of Fluid Mechanics, vol. 38, 2006, pp. 129-157
[27] J. X. Liu, "Modeling and analysis on aerodynamic heating for hypersonic glide vehicle," ChangSha, NUDT, 2008